

Supplementary material

SD-Net: Spatially-Disentangled Point Cloud Completion Network

Paper ID: 111

ACM MM 2023

Overview

This supplementary material consists of the following sections:

- In Section **A**, we present more qualitative comparison results for point cloud completion.
- In Section **B**, we present more specific quantitative results of our method and previous state-of-the-art methods on Shapenet-55/34.
- In Section **C**, we present the implementation details.
- In Section **D**, we provide detailed data preprocessing methods.
- In Section **E**, we present the complexity analysis of our method with previous methods.

A. More Qualitative Results

In Fig. 1, we provide more qualitative results for point cloud completion. It can be seen that our results can better infer missing structures and have smoother surfaces compared to other methods. In addition, we present the results of mesh reconstruction and error maps in Fig. 2 and Fig. 3, respectively, in order to better compare the smoothness and uniformity of distribution between our method and other methods in the completion results.

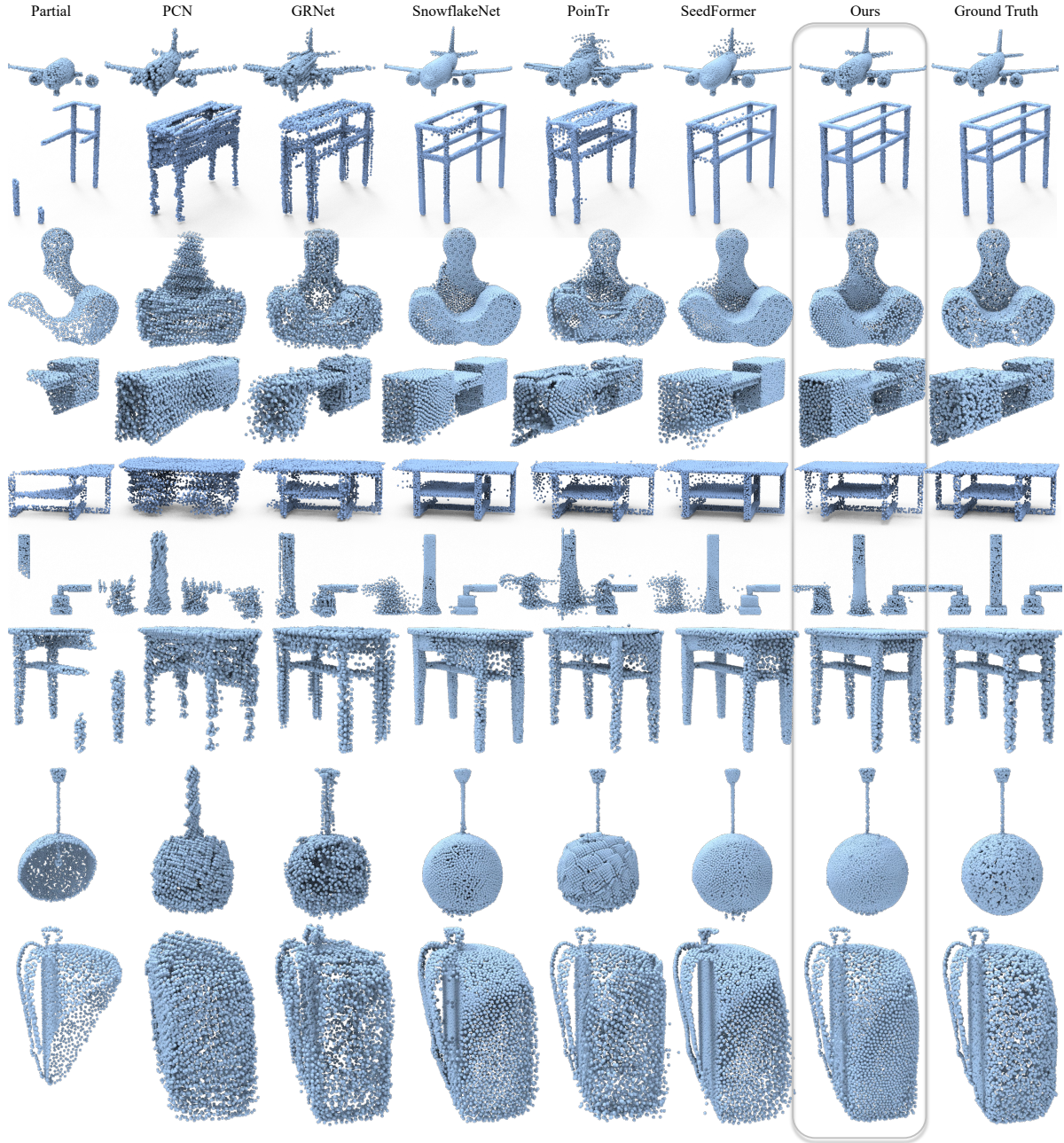


Figure 1. More qualitative results on the ShapeNet-55 dataset. Our SDNet is able to preserve the richest details and also outperforms the other state-of-the-art point cloud completion methods in recovering missing structures.

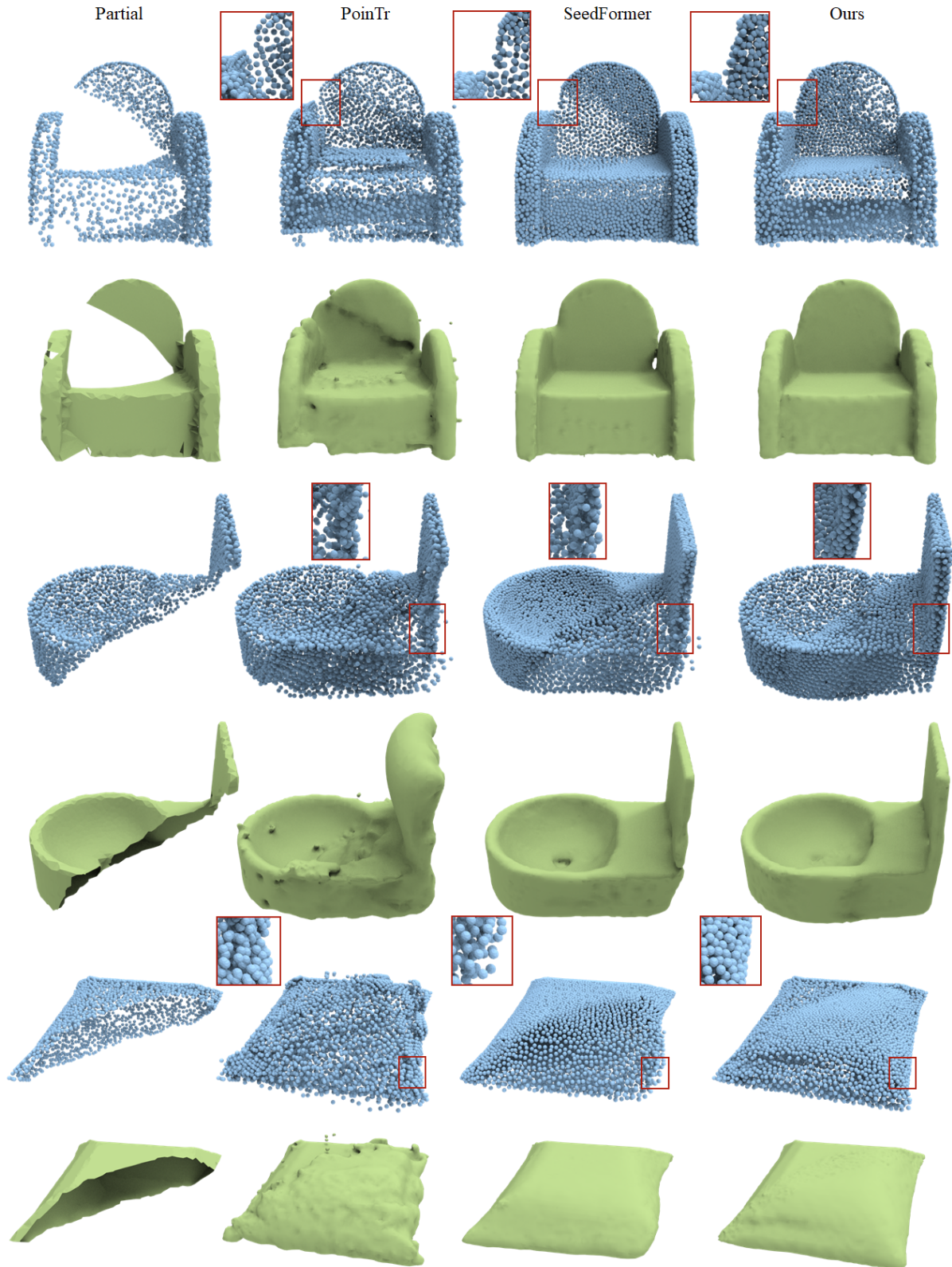


Figure 2. Comparing point cloud completion results and reconstructed 3D meshes using different methods. Clearly, our method outperforms others on the local details, contributing a better surface reconstruction.

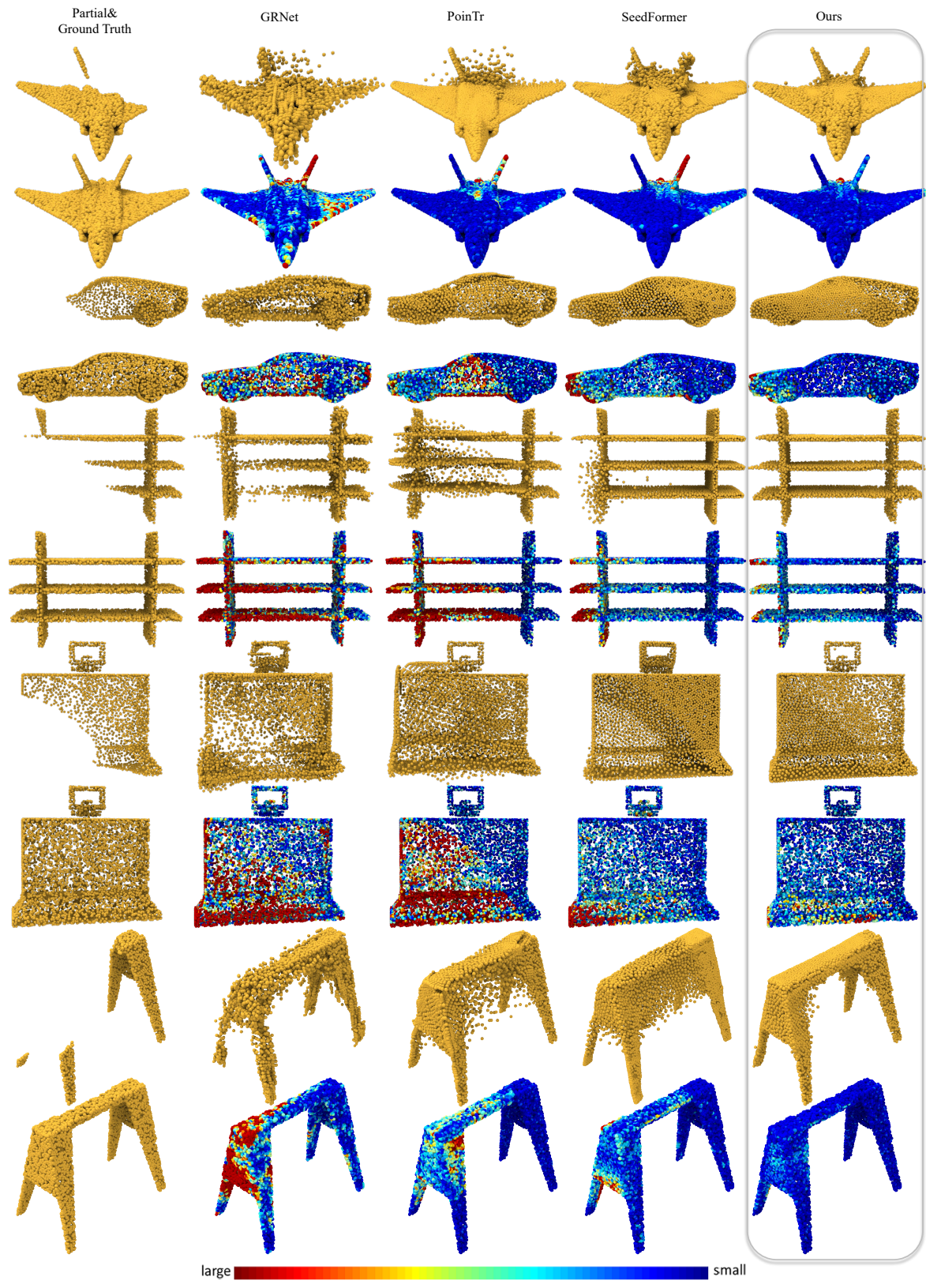


Figure 3. Comparing point cloud completion results using different methods. We also show the associated error maps, where the colors reveal the nearest distance for each target point to the point set generated by each method.

B. Detailed Quantitative Results

Detailed results on ShapeNet-34. In Table 1, we compared the detailed results of the previous state-of-art methods with our method for each category in ShapeNet-34 dataset at three different difficulties. The best results are marked in bold. We can clearly see that our method outperforms the previous methods at any difficulty for almost all 34 categories.

Detailed results on ShapeNet-55. In Table 2, we show the detailed results of the previous state-of-art methods and our method for each category in ShapeNet-55 dataset at three different difficulties. The best results are marked in bold. We can clearly see that our method outperforms the previous methods at any difficulty for all 55 categories.

Table 1. Detailed results under $CD-\ell_2$ (multiplied by 1000) for the novel objects on ShapeNet-34. *S.*, *M.* and *H.* stand for the simple, moderate and hard settings.

CD- ℓ_2 ($\times 1000$)	FoldingNet [6]			PCN [8]			TopNet [3]			GRNet [5]			SnowflakeNet [4]			PoinTr [7]			Ours-SDNet		
	S.	M.	H.	S.	M.	H.	S.	M.	H.	S.	M.	H.	S.	M.	H.	S.	M.	H.	S.	M.	H.
bag	2.15	2.27	3.99	2.48	2.46	3.94	2.08	1.95	4.36	1.47	1.88	3.45	0.67	1.08	1.82	0.96	1.34	2.08	0.53	0.84	1.37
basket	2.37	2.20	4.87	2.79	2.51	4.78	2.46	2.11	5.18	1.78	1.94	4.18	0.78	1.16	2.48	1.04	1.40	2.90	0.59	0.84	1.97
birdhouse	3.27	3.15	5.62	3.53	3.47	5.31	3.17	2.97	5.89	1.89	2.34	5.16	0.95	1.46	2.78	1.22	1.79	3.45	0.77	1.18	2.47
bowl	2.61	2.30	4.55	2.66	2.35	3.97	2.46	2.16	4.84	1.77	1.97	3.90	0.77	1.15	2.03	1.05	1.32	2.40	0.62	0.77	1.47
camera	4.40	4.78	7.85	4.84	5.30	8.03	4.24	4.43	8.11	2.31	3.38	7.20	1.27	2.30	4.31	1.63	2.67	4.97	1.05	1.81	3.84
can	1.95	1.73	5.86	1.95	1.89	5.21	2.02	1.70	5.82	1.53	1.80	3.08	0.62	0.94	1.73	0.80	1.17	2.85	0.57	0.80	1.64
cap	6.07	5.98	11.49	7.21	7.14	10.94	4.68	4.23	9.17	3.29	4.87	13.02	1.29	3.10	7.37	1.40	2.74	8.35	0.50	1.35	4.57
dishwasher	2.09	1.80	4.55	2.45	2.09	3.53	2.51	1.77	4.72	1.79	1.70	3.27	0.67	0.89	1.66	0.93	1.05	2.04	0.58	0.67	1.47
earphone	6.86	6.96	12.77	7.88	6.59	16.53	5.33	4.83	11.67	4.29	4.16	10.30	2.29	4.01	9.61	2.03	5.10	10.69	1.59	2.42	6.71
helmet	4.86	5.04	8.86	6.15	6.41	9.16	4.89	4.86	8.73	3.06	4.38	10.27	1.74	2.96	5.87	1.86	3.30	6.96	1.15	2.24	4.73
keyboard	0.98	0.96	1.35	1.07	1.00	1.23	0.79	0.77	1.55	0.73	0.77	1.11	0.38	0.46	0.63	0.43	0.45	0.63	0.28	0.32	0.46
mailbox	2.20	2.29	4.49	2.74	2.68	4.31	2.35	2.20	4.91	1.52	1.90	4.33	0.83	1.36	2.43	1.03	1.47	3.34	0.55	0.95	2.11
microphone	2.92	3.27	8.54	4.36	4.65	8.46	3.03	3.20	7.15	2.29	3.23	8.41	1.63	2.40	5.18	1.25	2.27	5.47	0.75	1.43	4.12
microwaves	2.29	2.12	5.17	2.59	2.35	4.47	2.67	2.12	5.41	1.74	1.81	3.82	0.72	0.96	1.78	1.01	1.18	2.14	0.64	0.75	1.56
pillow	2.07	2.11	3.73	2.09	2.16	3.54	2.08	2.05	4.01	1.43	1.69	3.43	0.55	0.86	1.75	0.92	1.24	2.39	0.56	0.72	1.49
printer	3.02	3.23	5.53	3.28	3.60	5.56	2.90	2.96	6.07	1.82	2.41	5.09	0.87	1.65	2.72	1.18	1.76	3.10	0.69	1.17	2.29
remote	0.89	0.92	1.85	0.95	1.08	1.58	0.89	0.89	2.28	0.82	1.02	1.29	0.32	0.47	0.67	0.44	0.58	0.78	0.27	0.39	0.57
rocket	1.28	1.09	2.00	1.39	1.22	2.01	1.14	0.96	2.03	0.97	0.79	1.60	0.36	0.57	1.05	0.39	0.72	1.39	0.29	0.52	0.95
skateboard	1.53	1.42	1.99	1.97	1.78	2.45	1.23	1.20	2.01	0.93	1.07	1.83	0.48	0.77	1.21	0.52	0.80	1.31	0.29	0.55	0.95
tower	2.25	2.25	4.74	2.37	2.40	4.35	2.20	2.17	5.47	1.35	1.80	3.85	0.67	1.12	2.20	0.82	1.35	2.48	0.57	0.95	1.91
washer	2.58	2.34	5.50	2.77	2.52	4.64	2.63	2.14	6.57	1.83	1.97	5.28	0.75	1.07	2.23	1.04	1.39	2.73	0.61	0.81	2.03
mean	2.79	2.77	5.49	3.22	3.13	5.43	2.65	2.46	5.52	1.84	2.23	4.95	0.88	1.46	2.92	1.05	1.67	3.45	0.64	1.02	2.32

Table 2. Detailed results on ShapeNet-55. *S.*, *M.* and *H.* stand for the simple, moderate and hard settings.

CD- ℓ_1 ($\times 1000$)	PCN [8]			GRNet [5]			SnowflakeNet [4]			PoinTr [7]			SeedFormer [11]			Ours-SDNet		
	S.	M.	H.	S.	M.	H.	S.	M.	H.	S.	M.	H.	S.	M.	H.	S.	M.	H.
airplane	16.25	16.4	17.47	13.92	14.37	15.90	9.01	10.00	11.74	7.89	8.68	10.89	7.93	8.99	11.16	6.98	7.36	9.51
bag	24.71	25.7	29.96	19.70	21.21	24.88	12.77	14.26	17.38	11.50	12.52	16.67	11.34	12.87	16.08	9.73	10.33	13.99
basket	25.51	26.3	31.96	23.35	24.35	27.83	15.52	16.81	20.58	13.83	14.60	18.80	14.28	15.45	19.39	11.76	11.94	15.88
bathtub	24.82	25.7	29.10	21.17	22.53	25.50	13.69	15.50	18.55	12.70	13.94	17.30	12.50	14.27	17.80	10.86	11.44	14.76
bed	30.24	31.6	35.83	21.36	23.25	27.78	14.79	16.68	21.08	13.27	14.89	19.95	13.24	14.94	19.24	11.21	12.16	16.55
bench	18.99	19.3	21.22	16.29	16.83	18.56	10.97	11.79	13.58	9.58	10.06	12.22	9.85	10.55	12.60	8.16	8.09	10.38
birdhouse	31.93	33.9	39.26	23.29	25.78	31.53	16.69	19.20	24.54	15.46	17.48	23.98	14.75	17.16	22.58	12.91	14.36	20.42
bookshelf	29.16	30.0	32.03	20.40	22.17	25.76	14.95	16.83	20.69	13.42	14.99	19.42	13.29	15.00	19.10	11.38	12.30	16.42
bottle	18.93	20.9	25.54	17.73	19.22	21.98	10.71	12.81	15.96	9.73	11.96	15.85	9.81	12.13	15.66	8.38	9.78	13.44
bowl	25.14	25.7	29.88	23.72	24.56	27.30	15.08	16.23	19.67	14.01	14.67	18.27	13.88	14.77	18.30	11.54	11.31	14.71
bus	19.88	20.5	21.41	17.94	18.61	19.57	12.23	13.31	14.61	10.64	11.40	13.01	11.41	12.53	13.95	9.45	9.65	11.42
cabinet	22.43	23.2	25.77	21.01	21.79	23.78	14.88	15.83	17.98	12.76	13.29	16.04	13.99	14.90	17.32	11.18	11.18	13.85
camera	35.00	37.0	44.08	23.48	27.15	33.96	16.89	20.58	27.26	15.64	19.40	27.25	14.54	18.40	25.21	13.22	16.30	22.85
can	23.14	25.6	33.39	22.85	24.76	28.30	14.57	16.83	20.37	12.99	15.17	19.44	13.58	16.01	19.46	11.20	12.58	16.19
cap	23.10	25.7	32.70	19.67	20.60	23.52	12.06	13.47	17.28	11.65	13.04	17.45	10.66	11.99	16.87	9.12	9.63	14.78
car	22.96	23.9	24.87	20.91	21.82	23.08	16.02	17.31	19.07	13.59	14.98	17.36	14.60	16.23	18.50	11.91	12.70	15.20
cellphone	15.91	16.8	18.34	16.06	16.60	17.46	10.85	11.69	12.86	9.51	9.89	11.29	10.14	11.04	12.26	8.22	8.21	9.78
chair	22.67	24.2	27.97	18.62	20.30	24.10	12.19	13.88	17.65	11.01	12.35	17.02	10.86	12.54	16.58	9.35	10.17	14.34
clock	24.47	25.1	28.72	20.61	21.87	24.71	14.04	15.48	18.41	12.43	13.45	17.08	12.57	13.96	17.08	10.57	11.02	14.45
dishwasher	22.20	23.9	28.77	22.29	23.18	26.41	14.58	15.58	19.54	12.90	13.56	17.47	13.86	14.64	18.10	11.18	11.10	15.15
display	21.83	22.8	25.66	18.61	19.75	22.41	12.58	14.01	16.72	11.12	11.91	15.08	11.23	12.49	15.42	9.44	9.74	12.87
earphone	29.70	30.5	42.41	19.78	22.24	29.80	14.39	16.76	23.42	13.49	16.36	25.90	12.38	14.67	21.65	11.87	13.55	19.22
faucet	28.54	30.4	36.33	16.81	19.63	25.68	11.12	14.24	20.28	10.81	14.25	21.96	9.27	12.43	18.89	9.04	11.51	17.82
file	24.56	25.8	29.20	21.61	22.82	26.14	15.35	16.66	19.96	13.22	14.16	18.11	14.36	15.60	18.89	11.46	11.90	15.58
flowerpot	31.63	32.9	37.21	24.11	26.14	30.59	17.91	19.79	24.23	15.28	17.48	22.95	15.60	17.54	22.44	13.21	14.51	19.61
guitar	10.78	10.9	12.47	9.93	10.45	11.84	6.09	6.84	8.11	5.62	6.22	7.95	5.49	6.30	7.74	4.79	5.22	6.72
helmet	33.95	37.0	44.04	24.76	28.39	36.08	17.51	20.93	27.82	15.45	19.09	27.38	15.01	18.41	25.81	13.31	15.75	23.34
jar	27.16	29.0	35.11	22.63	25.04	30.35	15.47	18.04	23.57	13.71	16.24	22.61	13.69	16.42	22.25	11.77	13.35	19.32
keyboard	15.64	15.9	16.63	15.11	15.28	15.73	10.34	10.90	11.93	8.74	8.86	9.82	9.56	10.15	11.10	7.56	7.35	8.50
knife	12.70	13.1	14.13	10.54	11.31	12.61	6.29	7.57	9.11	6.01	7.26	9.36	5.51	6.92	8.61	5.09	5.96	7.85
lamp	27.45	29.9	34.96	16.46	19.88	26.64	10.66	13.87	20.03	9.87	13.24	20.44	8.65	11.81	17.97	8.27	10.58	17.07
laptop	15.87	16.4	19.10	16.83	17.01	18.19	11.10	11.73	13.09	9.67	9.67	11.53	10.37	10.95	12.55	8.41	8.14	9.98
loudspeaker	27.04	28.5	32.50	22.48	24.38	28.27	15.76	17.64	21.50	14.03	15.69	20.24	14.25	15.99	20.10	12.03	12.90	17.06
mailbox	21.74	23.8	30.30	15.45	17.97	24.69	9.48	11.83	18.78	9.13	11.34	18.51	8.48	10.95	17.60	7.63	9.25	16.59
microphone	25.98	28.6	33.58	14.99	18.89	26.93	10.55	14.47	21.12	9.92	13.91	21.98	8.92	12.46	19.39	7.99	11.35	18.15
microwaves	24.52	26.1	31.71	23.12	24.16	27.64	15.26	16.43	19.77	13.67	14.23	18.01	14.36	15.31	18.98	11.81	11.76	15.34
motorbike	25.24	25.6	27.40	19.44	20.52	22.63	16.02	17.26	19.80	13.44	15.41	19.52	13.81	15.68	18.63	12.00	13.23	16.64
mug	27.67	28.7	34.18	24.69	25.98	29.49	17.00	18.63	23.05	15.52	16.66	21.86	15.56	17.18	22.08	13.18	13.66	18.68
piano	27.08	28.1	33.47	20.88	22.20	26.07	14.60	16.07	19.66	13.20	14.39	19.00	13.17	14.68	18.95	10.97	11.50	16.04
pillow	23.26	24.5	29.67	20.88	22.21	25.44	12.80	15.02	18.59	12.57	13.91	17.81	11.55	13.65	18.13	10.51	11.42	15.40
pistol	18.78	18.9	20.93	14.57	15.32	17.24	10.60	11.85	14.28	9.61	11.03	14.51	9.48	11.01	13.76	8.38	9.35	12.27
printer	30.62	32.4	37.40	22.18	24.57	29.91	14.62	17.11	21.84	13.41	15.40	20.49	13.09	15.31	20.24	11.29	12.39	17.56
remote	17.59	18.5	20.76	16.02	17.07	18.40	10.41	11.68	13.09	9.50	10.57	12.16	9.52	10.86	12.41	8.19	8.52	10.25
rifle	14.59	14.6	15.74	11.25	11.98	13.76	7.75	8.85	10.68	7.11	8.23	10.49	6.92	8.24	10.18	6.23	7.10	9.15
rocket	15.88	16.8	18.38	11.68	12.96	14.95	7.47	9.40	12.10	6.80	8.82	11.86	6.52	8.60	11.32	6.02	7.44	10.43
skateboard	16.72	17.4	18.65	14.18	14.97	16.45	9.13	10.28	11.65	8.24	9.02	10.63	8.27	9.23	11.14	6.98	7.47	9.19
sofa	23.52	24.0	26.66	20.72	21.51	23.63	13.77	14.91	17.11	12.33	12.75	15.23	12.58	13.61	15.97	10.57	10.49	13.19
stove	24.66	26.1	30.25	21.22	22.61	26.68	14.49	16.01	19.39	12.75	13.99	17.81	13.38	14.75	18.18	10.96	11.59	15.39
table	20.76	21.4	24.27	17.61	18.57	21.20	11.94	13.02	15.45	10.55	11.19	13.95	10.99	11.97	14.72	9.09	9.19	11.94
telephone	15.64	16.5	17.96	15.85	16.41	17.35	10.84	11.63	12.70	9.40	9.70	11.04	10.13	10.96	12.15	8.18	8.10	9.66
tower	22.83	24.3	28.03	17.65	19.71	24.06	12.62	14.79	18.78	11.17	13.26	17.88	11.15	13.44	17.57	9.58	11.19	15.51
train	21.00	21.2	22.26	16.85	17.64	19.08	12.61	13.72	15.60	10.77	11.84	14.30	11.35	12.57	14.57	9.46	10.02	12.44
trash	25.73	27.1	32.70	23.97	25.37	28.99	17.09	18.82	22.72	14.98	16.47	21.32	15.76	17.61	22.08	12.89 </td		

C. Implementation Details

In this section, we will give the specific implementation details of the SDNet. We train our network on the PyTorch platform. For ShapeNet-55/34 dataset, the network is set to train with a batchsize of 48 for 200 epochs and the AdamW optimizer is used with the learning rate of 0.005, which is continuously decreased by a decay rate of 0.76 for every 20 epochs. The hyperparameter α , β and γ are all set to 1, which means that the model training will pay more attention to the generation of missing regions. If the input point cloud in the dataset has large noise, the values of α and γ can be increased appropriately. On the MVP dataset [1], we set the batch size as before but set the epoch to 100 and adopt the same learning rate and decay rate as VRCNet[1].

Feature Extractor. We use two cascaded set abstraction (SA) [2] and point transformer (PT) [10] to extract features from the partial point cloud. In order to save computational cost, we progressively use Farthest Point Sampling(FPS) to downsample the original partial point cloud (2,048 points) to 256 center points. The detailed network architecture is: $SA(C_{in} = 3, C_{out} = 128, N_{out} = 512) \rightarrow PT(C_{in} = 128, C_{out} = 128) \rightarrow SA(C_{in} = 128, C_{out} = 256, N_{out} = 256) \rightarrow PT(C_{in} = 256, C_{out} = 256)$, where C_{in} and C_{out} are the numbers of feature channels of the input and output point clouds, and N_{out} is the number of points after FPS.

Set Transformer. We employ a lightweight Geometry-aware Transformer [7] as our Set Transformer to convert the center point of the partial point cloud to the keypoint of the missing part. Due to the strong strength of MCM in point cloud generation, we set the numbers of blocks of the encoder and decoder in Set Transformer to 1 and 2 and the hidden dimensions are set to 256.

D. Dataset Preprocessing Details

The purpose of data preprocessing is to provide strong and effective supervision for the training process of SDNet. This allows the point clouds generated by the two sub-networks to be better disentangled spatially. In this section, we give detailed data preprocessing details, as shown in Algorithm 1.

Algorithm 1 Point Cloud Spatial Disentangle Algorithm

```

1: Input: Partial point cloud  $P = \{p_i\}_{i=1}^N$ , complete point cloud  $P_c = \{p_i\}_{i=1}^{N_c}$ , resolution  $\sigma$ 
2: Output: Ground truth for refining  $P_r = \{p_i\}_{i=1}^{N_r}$ , ground truth for missing  $P_m = \{p_i\}_{i=1}^{N_m}$ 
3: Initialization:  $N_r = N_m = 0$ , the dilation kernel  $D_r = D_m = (2, 2, 2)$ 
4: Voxelize the  $P$  and  $P_c$  with the same resolution  $r$  to obtain  $V_p^\sigma$  and  $V_c^\sigma$ 
5: for  $N_r < \frac{N_c}{2}$  do
6:   Increase the size of the dilation kernel:  $D_r = D_r + 1$ 
7:   Perform a dilation operation on  $V_p^\sigma$ :  $V_p^{\sigma'} = \text{dilation}(V_p^\sigma, D_r)$ 
8:    $P_r = (V_p^{\sigma'} \cap V_c^\sigma) \cap P_c$ ,  $N_r = \text{num}(P_r)$ 
9:    $V_m^\sigma = \neg V_p^\sigma \cap V_c^\sigma$ 
10:  for  $N_m < \frac{N_c}{2}$  do
11:    Increase the size of the dilation kernel:  $D_m = D_m + 1$ 
12:    Perform a dilation operation on  $V_m^\sigma$ :  $V_m^{\sigma'} = \text{dilation}(V_m^\sigma, D_m)$ 
13:     $P_m = (V_m^{\sigma'} \cap V_c^\sigma) \cap P_c$ ,  $N_m = \text{num}(P_m)$ 
14:  end for
15: end for
16: Grid sampling for data alignment:  $P_r = GS(P_r, \frac{N_c}{2})$ 
17: Grid sampling for data alignment:  $P_m = GS(P_m, \frac{N_c}{2})$ 

```

Specifically, for the ShapeNet-34/55 dataset, we set the ground truth points of the missing region and refine region to be half of the total points in the complete point clouds, i.e., 4096 points. This results in better data alignment and concatenation. Furthermore, to determine the most suitable voxelization resolution, we also performed an analysis on the dataset and the results are shown in Fig. 4. The blue column indicates the number of samples included in this category. The polylines of different colors represent the number of sampling points at different resolutions. The closer these polylines are to 4096, the better the precision. As points exceed 4096, downsampling is required. This process will inevitably lose the structure of existing points, which is not conducive to refinement. There will be more cracks at the connection point of the final completion result when the number of points is less than 4096, since a larger dilation kernel will increase the connection range. Additionally, we use Grid Sampling(GS) rather than FPS in order to avoid destroying the overall structure of the point cloud.

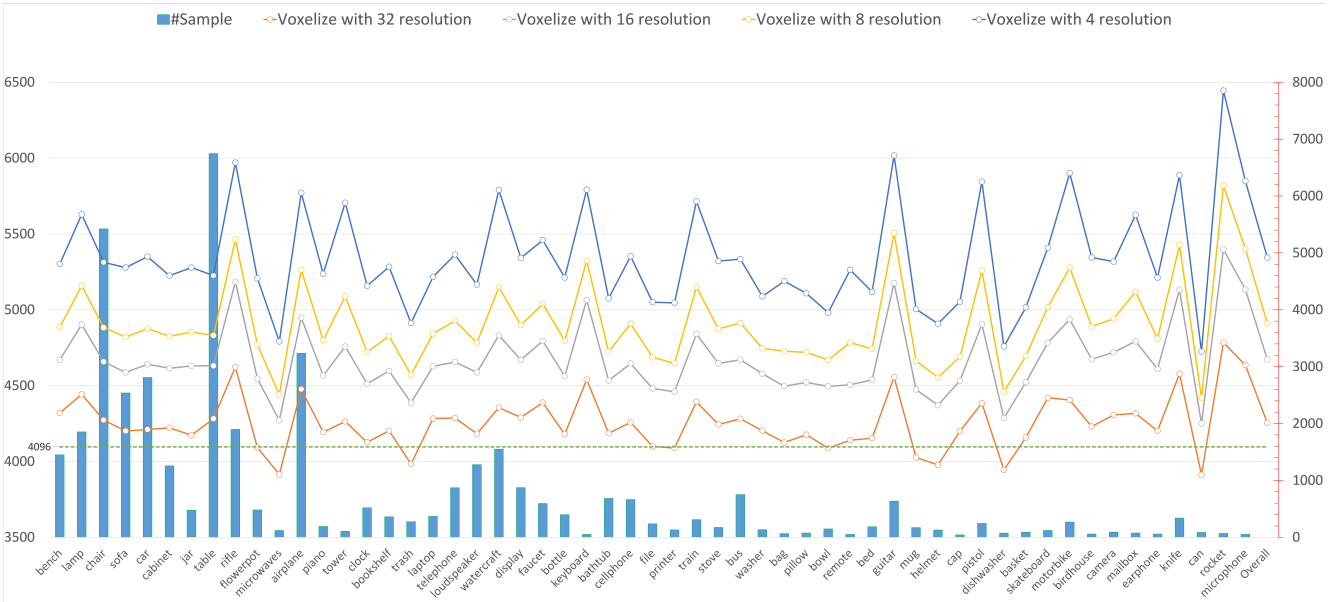


Figure 4. Specific ShapeNet-55 processing and analysis results. We provide the number of points obtained by voxelizing the point cloud at different resolutions and the number of samples included in the different categories.

E. Complexity Analysis

We provide a detailed complexity analysis in Table 3, including the number of parameters and theoretical computation cost (FLOPs) of different models under the ShapeNet-55 dataset. We also provide the overall Chamfer Distance of all categories in ShapeNet-55 and unseen 21 categories in ShapeNet-34 as references. Recent state-of-the-art methods have shown impressive performance gains, but often at the cost of increased time and space requirements. In contrast, our method achieves superior performance while maintaining low time and space overhead. Our approach strikes a balance between efficiency and effectiveness, with a focus on achieving the best possible performance without sacrificing practical considerations.

Table 3. Complexity analysis. We report the the number of parameter (Params) and theoretical computation cost (FLOPs) of our method and eight existing methods. We also provide the average Chamfer distances of all categories in ShapeNet-55 (CD_{55}) and unseen categories in ShapeNet-34 (CD_{34}) as references.

Models	Params	FLOPs	CD_{55}	CD_{34}
FoldingNet [6]	2.30 M	27.58 G	3.12	3.62
PCN [8]	5.04 M	15.25 G	2.66	3.85
TopNet [3]	5.76 M	6.72 G	2.91	3.50
PFNet [9]	73.05 M	4.96 G	5.22	8.16
GRNet [5]	73.15 M	40.44 G	1.97	2.99
PoinTr [7]	30.9 M	10.41 G	1.07	2.05
SnowflakeNet [4]	19.30 M	9.17 G	1.03	1.75
SeedFormer [11]	3.24 M	20.70 G	0.92	1.34
Ours	14.32 M	10.83 G	0.85	1.33

References

- [1] Liang Pan, Xinyi Chen, Zhongang Cai, Junzhe Zhang, Haiyu Zhao, Shuai Yi, and Ziwei Liu. Variational relational point completion network. In *Proceedings of the IEEE/CVF conference on computer vision and pattern recognition*, pages 8524–8533, 2021. [7](#)
- [2] Charles Ruizhongtai Qi, Li Yi, Hao Su, and Leonidas J Guibas. Pointnet++: Deep hierarchical feature learning on point sets in a metric space. *Advances in neural information processing systems*, 30, 2017. [7](#)
- [3] Lyne P Tchapmi, Vineet Kosaraju, Hamid Rezatofighi, Ian Reid, and Silvio Savarese. Topnet: Structural point cloud decoder. In *Proceedings of the IEEE/CVF Conference on Computer Vision and Pattern Recognition*, pages 383–392, 2019. [5](#), [10](#)
- [4] Peng Xiang, Xin Wen, Yu-Shen Liu, Yan-Pei Cao, Pengfei Wan, Wen Zheng, and Zhizhong Han. Snowflakenet: Point cloud completion by snowflake point deconvolution with skip-transformer. In *Proceedings of the IEEE/CVF international conference on computer vision*, pages 5499–5509, 2021. [5](#), [6](#), [10](#)
- [5] Haozhe Xie, Hongxun Yao, Shangchen Zhou, Jiageng Mao, Shengping Zhang, and Wenxiu Sun. Grnet: Gridding residual network for dense point cloud completion. In *Computer Vision–ECCV 2020: 16th European Conference, Glasgow, UK, August 23–28, 2020, Proceedings, Part IX*, pages 365–381. Springer, 2020. [5](#), [6](#), [10](#)
- [6] Yaoqing Yang, Chen Feng, Yiru Shen, and Dong Tian. Foldingnet: Point cloud auto-encoder via deep grid deformation. In *Proceedings of the IEEE conference on computer vision and pattern recognition*, pages 206–215, 2018. [5](#), [10](#)
- [7] Xumin Yu, Yongming Rao, Ziyi Wang, Zuyan Liu, Jiwen Lu, and Jie Zhou. Pointr: Diverse point cloud completion with geometry-aware transformers. In *Proceedings of the IEEE/CVF international conference on computer vision*, pages 12498–12507, 2021. [5](#), [6](#), [7](#), [10](#)
- [8] Wentao Yuan, Tejas Khot, David Held, Christoph Mertz, and Martial Hebert. Pcn: Point completion network. In *2018 International Conference on 3D Vision (3DV)*, pages 728–737. IEEE, 2018. [5](#), [6](#), [10](#)
- [9] Junchao Zhang, Jianbo Shao, Jianlai Chen, Degui Yang, Buge Liang, and Rongguang Liang. Pfnet: an unsupervised deep network for polarization image fusion. *Optics letters*, 45(6):1507–1510, 2020. [10](#)
- [10] Hengshuang Zhao, Li Jiang, Jiaya Jia, Philip HS Torr, and Vladlen Koltun. Point transformer. In *Proceedings of the IEEE/CVF international conference on computer vision*, pages 16259–16268, 2021. [7](#)
- [11] Haoran Zhou, Yun Cao, Wenqing Chu, Junwei Zhu, Tong Lu, Ying Tai, and Chengjie Wang. Seedformer: Patch seeds based point cloud completion with upsample transformer. In *Computer Vision–ECCV 2022: 17th European Conference, Tel Aviv, Israel, October 23–27, 2022, Proceedings, Part III*, pages 416–432. Springer, 2022. [6](#), [10](#)

The End